ELSEVIER

Journal of Power Sources 87 (2000) 21–27

JOURNAL OF POWER SOURCES

www.elsevier.com/locate/jpowsour

Numerical analysis of molten carbonate fuel cell stack performance: diagnosis of internal conditions using cell voltage profiles

F. Yoshiba [a,*], T. Abe [b], T. Watanabe [a]

[a] *Chemical Energy Engineering Department, Yokosuka Research Laboratory, Central Research Institute of Electric Power Industry, 2-6-1 Nagasaka, Yokosuka 240-0196, Japan*

[b] *Yokosuka Research Laboratory, Central Research Institute of Electric Power Industry, 2-6-1 Nagasaka, Yokosuka 240-0196, Japan*

Received 18 February 1999; received in revised form 13 July 1999; accepted 4 August 1999

Abstract

A numerical model to diagnose the internal conditions of a molten carbonate fuel cell (MCFC) has been developed to calculate both the temperature and performance of stacks. The performance of the stack is evaluated by applying a 'formula for MCFC performance' which has been derived from tests on single small cells with the same active components as the stack. Concerning the separator temperature and the cell performance, calculated results are compared with experimental data acquired during the operation of a 100-kW class stack. Good agreement is obtained. The applied numerical electric circuit model is modified to analyse the voltage distribution within each individual cell. The purpose of the model is to identify the cause of unexpected voltage differences within each cell during operation of a 100-kW class stack. Two causes are identified, namely, increase in the partial internal resistance (IR) and insufficient supply of fuel gas to the cell. The calculated cell voltage distribution and the observed voltage difference for a given cell exhibit similar behaviour.

Keywords: Molten carbonate fuel cell (MCFC); Large stack; Numerical analysis; Temperature profile; Electric circuit model; Cell voltage profile

1. Introduction

Molten carbonate fuel cells (MCFCs) are expected to be used as power-generation systems with high efficiency and low NO_x and SO_x emissions. It is anticipated that the technology will be introduced into practical use as either a centralized power station or a decentralized power plant.

The authors' research group has tested small single cells, as well as both 10- and 100-kW class large stacks. In these tests, the characteristics of the stacks have been evaluated by carrying out measurements of the individual cell voltages and the separator temperature, as well as by conducting analyses of the composition of the inlet and the outlet gases by means of gas chromatography. With respect to electricity generation, however, various complicated factors are intertwined, such as mass and heat transfer, chemical reactions, and electrical interaction. Thus, a numerical analysis model is required for evaluating stack performance.

Sampath et al. [1] have developed a numerical analysis model to calculate the current distribution in an isothermal single cell. Wolf and Wilemski [2] have studied the temperature distribution in a non-isothermal single cell by applying a simplified model for cell performance. Watanabe and Nikai [3] have analysed the cooling effect of cathode gas by assuming the MCFC to be parallel to the heating panel. Based on similar assumptions, Cao and Masubuchi [4] calculated the dynamic characteristics of the temperature distribution in single cells. Kobayashi et al. [5] and Fujimura et al. [6] analysed single cell and stack temperature profiles with respect to mass transfer during the generation of the reaction, and applied a thin-film cylindrical-pore model to study the relation between current density and cell voltage (j–V relation).

The j–V relation determines the rate of generated heat and the rate of chemical reaction. Therefore, the purpose of this study is to make an exact statement of the j–V relation. In previous work [7,8], the authors' research group has derived a 'formula for MCFC performance', which has been determined under various gas and temperature conditions, using small single cells which have the

* Corresponding author. Tel.: +81-468-56-2121; fax: +81-468-56-3346; e-mail: yoshiba@criepi.denken.or.jp

0378-7753/00/$ - see front matter
PII: S0378-7753(99)00352-3

same active components as the stack. On the basis of this formula, the dynamic characteristics of a single cell have been analysed [9].

The authors have examined [10,11] the performance and temperature profiles of 10- and 100-kW class stacks with a 1-m^2 reactive area. During operation of 100-kW class stacks, an unexpected cell voltage distribution in each individual cell was observed. This phenomenon is presumably caused either by the maldistribution of fuel gas to individual cells or by the internal resistance (IR) distribution within each cell — neither of which was observed during tests on single cells. The existing method is inappropriate for analysing the internal conditions of a MCFC-stack with such abnormal features and, therefore, a new advanced numerical analysis model is required.

This report describes the development of a new advanced MCFC-stack model combined with an electric circuit model using the 'formula for MCFC performance'. The approach is accurate, especially for the j–V relation at low hydrogen concentrations [12], and makes allowance for anomalous voltage distribution. The model has been developed for co-flow type stacks, i.e., fuel gas and oxidant gas flow in the same direction.

Variables and constants

C	molar concentration (mol/m^3)
C_p	specific heat at constant pressure (J/kg K)
E	electromotive force (V)
F	Faraday constant (C/mol)
h	coefficient of heat transfer (W/m^2 K)
I	load current (A)
J	current density (A/m^2)
K_p	equilibrium constant
L	gas channel length (m)
M	molar weight (kg/mol)
p	partial pressure (Pa)
R_{ir}	internal resistance (Ω m^2)
R_a	anode reaction resistance (Ω m^2)
R_c	cathode reaction resistance (Ω m^2)
R_s	electrical resistance of separator (Ω)
r_{GEN}	generating reaction rate (mol/m^2 s)
r_{SHIFT}	shift reaction rate (mol/m^3 s)
T	temperature (K)
u	gas velocity (m/s)
V	cell voltage (V)
Y	cell width (m)
α_{GEN}	formation enthalpy of H_2O (J/kg)
α_{SHIFT}	enthalpy of shift reaction (J/kg)
δ	thickness of channel and of each component (m)
ε	thickness of corrugated plate (m)
σ	Stefan–Boltzmann constant (W/m^2 K^4)
λ	heat conductivity (W/m K)
τ	residence time of anode gas in anode channel (s)

Subscripts

a	anode
c	cathode
e	electrolyte and electrode
s	separator
w	corrugate

The subscripts of a gas, such as H_2, CO_2, etc., specify each type of gas, and two following subscripts refer to the relation between each component.

2. System modelling

The configuration of a single cell in a MCFC is presented in the upper part of Fig. 1. The single cell is comprised of separator plates, corrugated plates, current collectors, electrodes (cathode and anode), and electrolyte. Fuel and oxidant gas flow through the anode and cathode side channels and pass the corrugated plates. O_2 and CO_2 in the oxidant gas react with electrons at the cathode and produce CO_3^{2-}. Due to the driving force of the concentration difference, the CO_3^{2-} moves within the electrolyte plate perpendicularly away from the cathode to the anode. At the anode, the H_2 in the fuel gas reacts with CO_3^{2-} and,

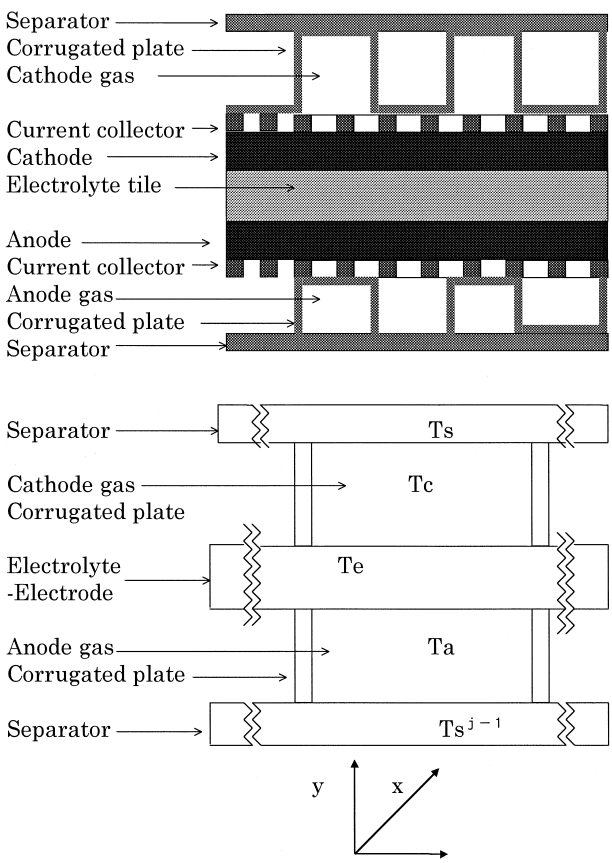

Cathode reaction $CO_2 + \frac{1}{2}O_2 + 2e^- \rightarrow CO_3^{2-}$

Anode reaction $H_2 + CO_3^{2-} \rightarrow H_2O + CO_2 + 2e^-$

Shift reaction $H_2 + CO_2 \leftrightarrow H_2O + CO$

Fig. 1. Conceptual structure of single cell and analysis model.

via an electrochemical reaction, CO_2, H_2O and electrons are produced. Electrons released from the reaction sites are collected by the current collector. They then pass the corrugated plates and reach the separator perpendicularly. The separators, located at the top and bottom, are connected to the loading equipment.

The heat produced in the electrochemical reaction is transferred to the anode and cathode gases by means of heat convection, whereas between electrodes and gases the heat is carried by mass exchange. The heat is also transported directly from the electrodes to the separator plates by means of radiation. A corrugated plate, located within the gas channel, also transmits the generated heat by means of conduction. The model is shown schematically in the lower part of Fig. 1. Here, electrolyte, electrode, and current collector appear together as one component.

3. Approximation and regulating equations

The following assumptions and approximations are applied to derive the basic equations.

(i) The analysis of each cell is one-dimensional in the gas flow direction (x-direction). The heat transfer between cells takes place through the separators in the stacking direction.

(ii) The density and characteristic values of anode and cathode gases are exclusively facts regarding the gas composition.

(iii) The heat conduction of the gases and the electrolyte plates is negligible.

3.1. Mass balance

The changing mole-flow rates of each gas and mixed gas are written as follows:Cathode gas:

$$\delta_c \frac{dC_{c,k}u_c}{dx} = Ar_{GEN} \quad C_c\delta_c\frac{du_c}{dx} = -\frac{3}{2}r_{GEN} \tag{1}$$

where k represents the gas compositions CO_2, O_2, N_2; coefficient A is -1 for CO_2, $-1/2$ for O_2, and 0 for N_2.Anode gas:

$$\delta_a \frac{dC_{a,l}u_a}{dx} = Br_{GEN} + C\delta_a r_{SHIFT} \quad C_a\delta_a\frac{du_a}{dx} = r_{GEN} \tag{2}$$

where l represents the gas compositions H_2, CO_2, H_2O, CO; coefficient B is -1 for H_2, 1 for CO_2 and H_2O, 0 for N_2; coefficient C is 1 for H_2 and CO_2, and -1 for H_2O and CO, respectively.

The generating reaction rate is expressed as follows:

$$r_{GEN} = \frac{J(x)}{2F} \tag{3}$$

The shift reaction of the anode gas is expressed as follows:

$$\frac{1}{K_p(T_a)} = \frac{(C_{H_2}+X)(C_{CO_2}+X)}{(C_{H_2O}-X)(C_{CO}-X)} \tag{4}$$

where X denotes the rate of concentration change in the shift reaction. As is known, the residence time concerning the mesh width in the x-direction is short, so the shift reaction cannot be in equilibrium as given by Eq. (4). By using the variable coefficient parameter $\alpha(<1)$, the shift reaction rate is expressed as follows:

$$r_{SHIFT} = \alpha\frac{X}{\tau} = \alpha X\frac{u_a}{\Delta x} \tag{5}$$

3.2. Energy equation

Energy conservation equations for a cell j are written as follows: the subscripts $j-1$ and $j+1$ denote adjoining cells.Cathode gas:

$$\delta_c\sum_k\left(\frac{d\rho_k Cp_k u_c T_c}{dx}\right) = q_{sc}+q_{ec}+q_{wc}-q_{GENec} \tag{6}$$

where k represents the gas compositions CO_2, O_2 and N_2.Anode gas:

$$\delta_a\sum_t\left(\frac{d\rho_t Cp_t u_a T_a}{dx}\right) = q_{sa}^{j-1}+q_{ea}+q_{wa}-q_{GENea}+q_{SHIFT} \tag{7}$$

where l represents the gas compositions H_2, CO_2, H_2O and CO.Electrolyte within electrode plate:

$$q_{GEN}-q_{ec}-q_{ea}-q_{es}-q_{es}^{j-1}-q_{ew}-q_{ew}^{j-1}+q_{GENec}+q_{GENea}=0 \tag{8}$$

Separator plate:

$$-\lambda_s\delta_s\frac{d^2T_s}{dx^2} = q_{se}+q_{se}^{j+1}+q_{sw}+q_{sw}^{j+1}-q_{sc}-q_{sa}^{j+1} \tag{9}$$

The convection heat-transfer term in the energy equation is expressed as follows:

$$q_{sc}=h_{sc}(T_s-T_c) \quad q_{ec}=h_{ec}(T_e-T_c)$$
$$q_{sa}=h_{sa}(T_s-T_a) \quad q_{ea}=h_{ea}(T_e-T_a) \tag{10}$$

where the heat-transfer coefficient is expressed as $h=Nu(\lambda/\delta)$. The value $Nu=3.0$ has been selected for this analysis.

The radiation term stating the heat transfer from the electrolyte plate to the separator plate is expressed and approximated as follows:Cathode side:

$$q_{es}=\sigma\phi_c\left(T_e^4-T_s^4\right)\approx 4\sigma\phi_c T^{*3}(T_e-T_s)$$

Anode side:

$$q_{es}=\sigma\phi_a\left(T_e^4-T_s^4\right)\approx 4\sigma\phi_a T^{*3}(T_e-T_s) \tag{11}$$

where ϕ_c and ϕ_a are the geometric factors in each gas channel, and T^* represents the temperature, viz., 923 K. With respect to the heat conduction of the corrugated plates and the convection heat transfer from the corrugated

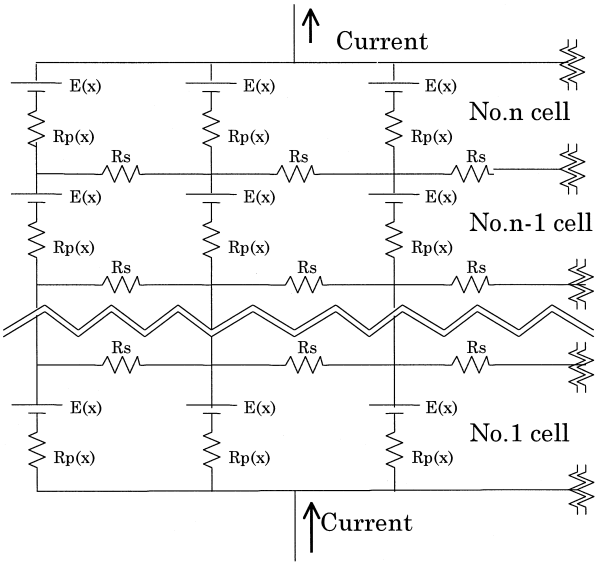

Fig. 2. Electric circuit model of MCFC $E(x)$, $R_p(x)$ are electromotive force and IR, respectively. R_s is the electric resistance of the separator.

plates to each gas, a heat transfer model is applied and the heat transfer is calculated exactly by:

$$\varepsilon\lambda\frac{\partial^2 T(y)}{\partial^2 y} - 2h_{we}\{T(y) - T_c\} = 0 \tag{12}$$

where y is the co-ordinate for the stacking direction.

The generated heat from the generating and shift reactions is expressed as:

$$q_{GEN} = \alpha_{GEN} r_{GEN} \quad q_{SHIFT} = \alpha_{SHIFT} r_{SHIFT} \tag{13}$$

The heat transfer by gas enthalpy in the generating reaction is written as:

$$q_{GENea} = \left(Cp_{H_2} M_{H_2} T_a - Cp_{CO_2} M_{CO_2} T_e - Cp_{H_2O} M_{H_2O} T_e\right) \times r_{GEN}$$

$$q_{GENec} = \left(Cp_{CO_2} M_{CO_2} T_c + \frac{1}{2} Cp_{O_2} M_{O_2} T_c\right) r_{GEN} \tag{14}$$

3.3. Current density profile and output voltage

Under ordinary operating conditions, the relation between cell voltage and current density in a MCFC can be written as:

$$V \cong E(x) - \{R_{ir}(x) + R_a(x) + R_c(x)\} J(x)$$
$$= E(x) - R_p(x) J(x) \tag{15}$$

The Nernst voltage and the cell resistance are [7,8,10,12]:

$$E = E^0 + \frac{RT_e}{2F} \ln \frac{p_{H_2a}\, p_{CO_2c}\, p_{O_2c}^{1/2}}{p_{CO_2a}\, p_{H_2O}} \tag{16}$$

$$R_{ir} = AR \exp\left(-\frac{\Delta HR}{RT_e}\right) \tag{17}$$

$$R_a = AR_{an} T_e \exp\left(-\frac{\Delta H_a}{RT_e}\right) P_{H_2a}^{-0.5} \tag{18}$$

$$R_c = A_D T_e \exp\left(-\frac{\Delta H_{O_2}}{RT_e}\right) P_{O_2}^{-0.75} P_{CO_2}^{0.5} + A_E T_e \exp\left(-\frac{\Delta H_{CO_2}}{RT_e}\right) P_{CO_2}^{-1.0} \tag{19}$$

where AR, ΔHR denote the frequency coefficient of IR and the activation energy, respectively. ΔH_a, ΔH_{O_2}, ΔH_{CO_2} give an indication of the activation energy of each gas, and AR_{an}, A_D, A_E are the coefficients derived from tests on single cells which have a reactive area of 100 cm^2.

The following relationship for the case of constant cell voltage in gas flow direction is derived from Eq. (15).

$$V = \left\{\int_0^l \frac{E(x)}{R_p(x)} dx - I\right\} \Big/ \int_0^l \frac{1}{R_p(x)} dx \tag{20}$$

It is impossible to calculate the cell voltage with Eq. (15) for the case of multiple cell voltage profiles in the gas-flow direction. In order to calculate the cell voltage profiles, an electric circuit model is applied to the MCFC stack, as presented in Fig. 2. It is possible to calculate the cell voltage and current profiles of each cell by applying Kirchhoff's law, which considers the stack to be a combination of small cells. By using the equations for calculating mass (Eqs. (1) and (2)), energy (Eqs. (6)–(9)), current and voltage (Eq. (20)), or by applying an electric circuit model as shown in Fig. 2, the profiles for temperature, gas concentration, current density and cell voltage of each cell in the stack can be determined.

4. Numerical analysis method and calculating conditions

In the numerical analysis, up-wind difference approximation is applied for the first derivative of the mass and the energy equation, and centre difference approximation for the second derivative. To calculate the temperature profile, a large matrix is made and the Gauss–Jordan method is applied. Table 1 presents characteristic values and cell sizes. The parameters indicated in Table 2 are

Table 1
Cell characteristics and sizes

Parameter	Values
λ_s	22.0 [W/m K]
h_{sa}, h_{ea}, h_{wa}	593.1 [W/m^2 K]
h_{sc}, h_{ec}, h_{wc}	91.1 [W/m^2 K]
ϕ_c	0.43
ϕ_a	0.25
R_s	2.5×10^{-6} [Ω]
δ_a	1.0×10^{-3} [m]
δ_c	2.0×10^{-3} [m]
L	0.56 [m]

Table 2
Coefficient of formula for MCFC performance

	Value [unit]
AR	6.43×10^{-3}
ΔHR	-25.5×10^{3} [J/mol]
AR_{an}	8.11×10^{-9}
ΔH_a	-74.4×10^{3} [J/mol]
A_D	2.10×10^{-10}
ΔH_{O_2}	-101.0×10^{3} [J/mol]
A_E	1.58×10^{-5}
ΔH_{CO_2}	-7.12×10^{3} [J/mol]

used for the coefficient of the 'formula for MCFC-performance'; these have been derived from single cells constructed from the same components as the stack.

During the accuracy investigation, a mesh width of 10 mm is selected. The results of single-cell tests show that the shift reaction reaches equivalence in less than 1 s, but as the reaction time is not known, 0.25 is taken for α to achieve a delay of the shift reaction.

5. Analyses of 100-kW class stack performance

5.1. Evaluation of experimental results for stack performance, temperature profiles and required gas-flow rate

5.1.1. Cell voltage and temperature profile in stack

In Fig. 3, a comparison is made of the calculated and experimental data for the voltage and the temperature profiles of each cell within the lower module of a 100-kW class stack which consists of 51 cells. By applying numerical analysis to evaluate the temperature profile in the stack, a fixed temperature condition is selected at the end separators. The calculated voltage of each cell is in accordance with the experimental data, except in the case of low-voltage cells. The calculated temperature profile is also consistent with the corresponding experimental data. These results prove that the constructed model is applicable as an analysis method for the internal condition of the stack. The temperature profile, indicated by a black continuous line in Fig. 3, is calculated on the assumption that an adiabatic condition exists at the end separators. Agreement of the calculated temperature with the test results means that the stack has been operated under an adiabatic condition of the end separators.

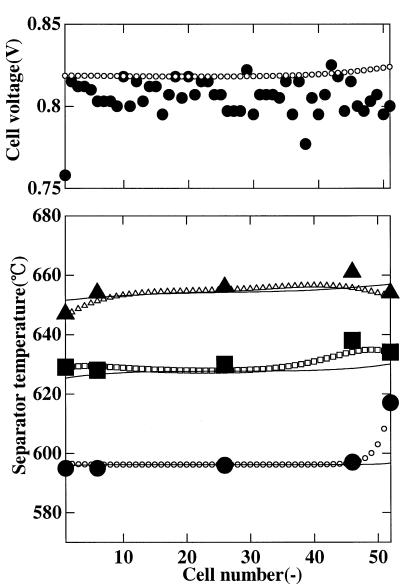

Fig. 3. Comparison of calculated cell voltage and separator temperature profile for 100-kW class stack. Operating pressure = 0.49 MPa; current density = 1500 A/m^2; fuel utilization = 80%; overall oxidant utilization = 30%; air/CO_2 = 70/30; cathode recycling ratio = 62%. Cell voltage: (●) experimental, (○) calculated. Experimental temperature (●) gas inlet, (■) center of cell, (▲) gas outlet. Calculated temperature: (○) gas inlet, (□) center of cell, (△) gas outlet. Continuous lines are calculated on assumption that an adiabatic condition exists at the end separator.

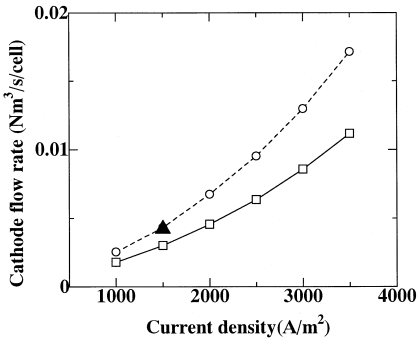

Fig. 4. Cathode flow rate vs. current density. Operating pressure = 0.49 MPa; fuel utilization = 80%; overall oxidant utilization = 30%; air/CO_2 = 70/30; reactive area = 1 m^2; anode/cathode inlet gas temperature = 595/600 K. Experimental: (▲) maximum temperature: 656°C. Calculated: (○) maximum temperature: 655°C, (□) maximum temperature: 680°C.

5.1.2. Cooling gas-flow rate at higher power density

To secure a longer lifetime for the MCFC stack, the maximum temperature must be adjusted to remain below the set value to avoid electrolyte loss by corrosion. Using the developed model, the required cathode gas flow rate of a coolant to control the maximum temperature is calculated under operating conditions of high output power density. The required gas-flow rate to maintain maximum separator temperatures of 928 and 953 K is shown in Fig. 4. The experimental gas-flow rate for a 100-kW class stack

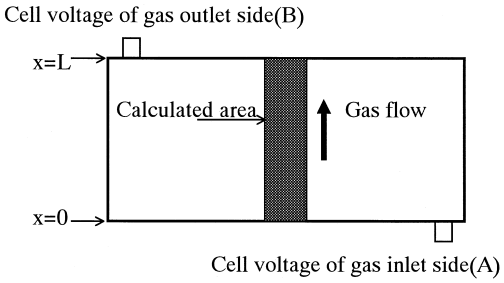

Fig. 5. Cell voltage measurement points.

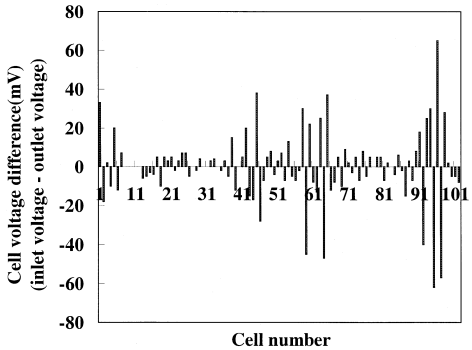

Fig. 6. Cell voltage difference observed during test of 100-kW class stack.

(1500 A/m^2) is also indicated. By applying this model, the total amount of cathode gas under high output operating conditions has been estimated.

5.2. Cell voltage difference in a 100-kW class stack

The measuring points for voltage in each individual cell within a 100-kW class stack are shown in Fig. 5. The measurement points are located at the gas inlet and outlet, respectively. The measured cell voltage differences between the gas inlet and outlet sides are presented in Fig. 6. These have been recorded during an operation time of 660 h [11]. Note that, if the voltage of a cell on the inlet side is lower than on the outlet side, the voltage of the adjoining cells on the inlet side is usually higher than on the outlet side. This is the first report of such cell voltage differences.

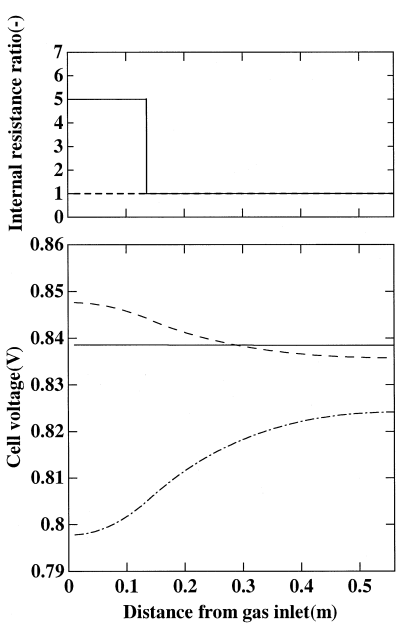

Fig. 7. Supposed IR and calculated cell voltage profiles in the case of IR trouble. IR value of ordinary cell is taken as unity. Internal resistance: (---) ordinary cell, (—) troubled cell. Cell voltage: (—) ordinary cell, (—·—·) troubled cell, (---) adjoining cell.

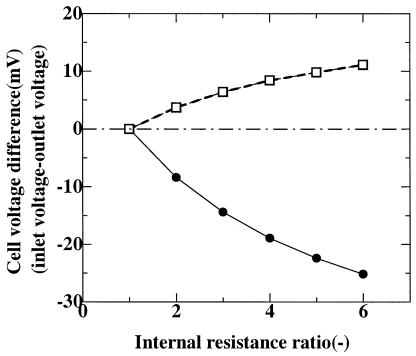

Fig. 8. Cell voltage deference vs. supposed IR ratio when IR of quarter the area of troubled cell at the gas inlet side is increased. IR ratio is unity in ordinary cell. (●) Troubled cell, (□) adjoining cell.

5.3. Factors causing voltage difference

To evaluate the cell voltage differences which have been observed in the test of a 100-kW class stack, two possible solutions regarding the influence on the cell voltage distribution within an individual cell are supposed, namely, a partial increase in IR, and an insufficient supply of fuel to a particular cell.

5.3.1. Distribution of cell voltage with partial IR-increase

To evaluate the cell voltage distribution in the case of IR-increase in a partial area, it is supposed that in one-quarter of the cell area (troubled cell) on the gas inlet side, the IR-increase was up to five times higher than in other areas. The IR-profile and the calculated cell voltage distribution of the troubled cell, the adjoining cells, and ordinary cells are presented in Fig. 7. The voltage of the troubled cell increases from the gas inlet side to the gas outlet side, while in the adjoining cells it decreases. The calculated cell voltage distribution indicates that the partial IR-increase could be responsible for the voltage difference between the gas inlet and outlet sides. The cell voltage difference of the troubled cell and the adjoining cells for various IR-values is shown in Fig. 8. With IR-increase, the

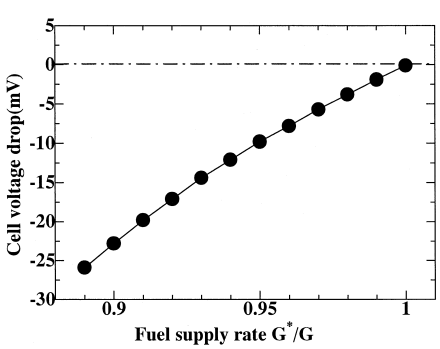

Fig. 9. Average cell voltage drop vs. rate of fuel supply in case of insufficient fuel supply. Current density = 1500 A/m^2; fuel utilisation = 80%. G^*: fuel flow rate of troubled cell, G: fuel flow rate of ordinary cell.

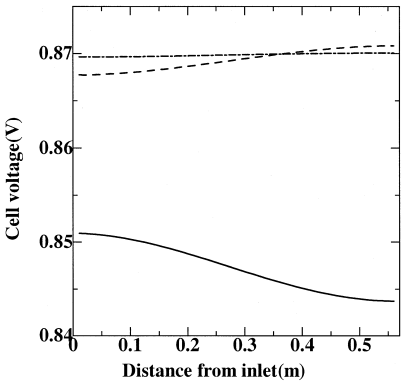

Fig. 10. Calculated cell voltage profile for insufficient supply of fuel in troubled cell. Supply of fuel cell = 0.9 (—·—·) ordinary cell, (—) troubled cell, (---) adjoining cell.

cell voltage difference between the troubled cell and adjoining cells increases as indicated in the figure.

5.3.2. Cell voltage distribution caused by insufficient supply of fuel gas

An insufficient supply of fuel gas triggers a decrease in cell voltage. The calculated voltage drop is shown in Fig. 9 and is based on the assumption that only one cell within the 100-kW stack is supplied with insufficient fuel gas. It is assumed that the fuel gas which is not supplied to the cell is redistributed to other cells in the stack. Since the cell voltage is distributed in the gas flow direction, as described below, the cell voltage discussed in Fig. 9 refers to the average voltage within each cell.

The calculated cell voltage distribution of the insufficiently supplied fuel cell (troubled cell) and adjoining cells is shown in Fig. 10 for a gas supply rate of 0.9. The cell voltage of the troubled cell decreases from inlet to outlet, whereas it increases in the adjoining cells. It is supposed that this voltage distribution is caused by an increase in the resistance of the anode reaction at the outlet side with a lower H_2 partial pressure. Not shown in Fig. 10 is the fact that the calculated results indicate that a greater insufficiency of fuel gas supply causes a greater difference in cell voltage.

6. Conclusions

(1) A numerical analysis model which can calculate the performance, temperature and current profiles, and cell voltage distribution of co-flow MCFC stacks has been developed. The calculated performance and temperature profile of the stack are in accordance with the experimental data, so that the constructed model is applicable for the internal condition analysis of a MCFC stack.

(2) Based on the above model, the required cathode gas flow rate is analysed for operating conditions of high-output power. The total amount of cathode gas, which is required to cool down a stack, is estimated for a current density which ranges from 1000 to 3500 A/m^2.

(3) Voltage distribution analysis suggests that an increase in the partial IR and an insufficient supply of fuel gas to a particular cell could be responsible the observed difference in cell voltage. It has also been established that such differences occur during operation of a 100-kW class stack. Greater increase in partial IR and greater insufficiency of fuel gas in a particular cell will result in a larger cell voltage difference.

References

[1] V. Sampath, A.F. Sammells, J.R. Selman, A performance and current distribution model for scaled-up molten carbonate fuel cells, Electrochem. Soc. 127 (1) (1980) 79–85.
[2] T.L. Wolf, G. Wilemski, J. Electrochem. Soc. 130 (1) (1983) 49–55.
[3] T. Watanabe, I. Nikai, Cooling characteristics of a molten carbonate fuel cell, JSME B 52 (481) (1986) 3335–3340.
[4] G. Cao, M. Masubuchi, Dynamic modeling of molten carbonate fuel cell and its dynamic response, JSME B 57 (535) (1991) 837–842.
[5] N. Kobayashi, H. Fujimura, K. Ohtsuka, Heat and mass transfer in a molten carbonate fuel cell: 1st report. Experimental and analytical investigation of fuel cell temperature distribution, JSME B 54 (505) (1988) 2568–2574.
[6] H. Fujimura, N. Kobayashi, K. Ohtsuka, Heat and mass transfer in a molten carbonate fuel cell: 2nd report. Analysis investigation of performance and temperature distribution in a cell stack, JSME B 57 (535) (1991) 825–830.
[7] Y. Mugikura, T. Abe, T. Watanabe, Y. Izaki, Analysis of performance of molten carbonate fuel cell: II. Development of a performance correlation equation, Denki Kagaku 60 (2) (1992) 124–130.
[8] H. Morita, Y. Mugikura, Y. Izaki, T. Watanabe, T. Abe, Analysis performance of molten carbonate fuel cell: IV. Performance formulation based on cathode reaction mechanisms, Denki Kagaku 63 (11) (1995) 1053–1060.
[9] T. Watanabe, E. Koda, Y. Mugikura, Y. Izaki, T. Watanabe, Development of molten carbonate fuel cell dynamic performance model, JSME B 58 (548) (1992) 1228–1233.
[10] Y. Mugikura, Y. Izaki, T. Watanabe, T. Abe, T. Shimizu, S. Sato, T. Matsuyama, Evaluation of a 10-kW class MCFC stack performance by a correlation equation, CRIEPI Report W93020, 1994.
[11] Y. Izaki, T. Watanabe, T. Abe, M. Tooi, T. Matsuyama, M. Hosaka, Power generating performance of 100-kW class MCFC stack, JSME B 61 (592) (1995) 12.
[12] H. Morita, Y. Mugikura, Y. Izaki, T. Watanabe, T. Abe, Analysis of performance of molten carbonate fuel cell: V. Formulation of anode reaction resistance, Denki Kagaku 65 (9) (1997) 740–746.